Proceedings of the 16th International Conference on Soil Mechanics and Geotechnical Engineering

doi:10.3233/978-1-61499-656-9-2129

Bored and screwed piles

Pieux forés et pieux vissés

R. Katzenbach & A. Schmitt
Institute and Laboratory of Geotechnics, Technische Universität Darmstadt, Germany

ABSTRACT

Piling is one of the most necessary and powerful construction techniques applied in geotechnical engineering. The efficiency of bored piles (where soil is retrieved) and screwed piles (where soil is displaced) results from the interaction between the performance of the drilling equipment and the modifications created by the drilling process to the soil characteristics. Although little is known yet on what in detail is happening during the pile installation, continuum models can provide a reliable tool to predict load capacities and load bearing behaviour of axially loaded piles. Numerical simulations based on the Finite-Element-Method (FEM) are presented to predict the bearing capacities of bored and screwed test piles in sand.

RÉSUMÉ

La fabrication des pieux est l'une des techniques de construction les plus essentielles et les plus puissantes qui est appliquée en géotechnique. L'efficacité des pieux forés (où le sol est remplacé) et des pieux vissés (où le sol est déplacé) résulte de l'interaction entre l'équipement de forage et les modifications des caractéristiques du sol dues au processus de forage. Bien que l'on connaisse peu ce qui se passe en détail pendant l'installation de pieu, les modèles de continuum peuvent fournir un outil fiable pour prévoir des capacités de charge et de comportement en charge des pieux axialement chargés. Des simulations numériques, basées sur la méthode des Eléments Finis (FEM), sont présentées pour prévoir les portances des pieux hélices et des pieux vissés en sable.

1 INTRODUCTION

Numerical models have been developed in order to predict the load settlement behaviour of 3 m long continuous flight auger piles (CFA-piles) and screwed piles (small scale tests) with an adjustable soil displacement (Katzenbach et al., 2004) in sand (Fig. 1 and 2). These models are presented together with the comparison of the computed results and the measured results obtained from pile testing.

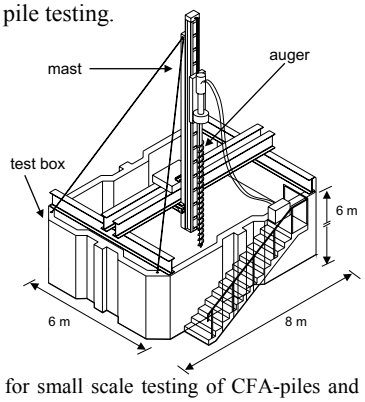

Figure 1. Setup for small scale testing of CFA-piles and soil-displacement piles (screwed piles)

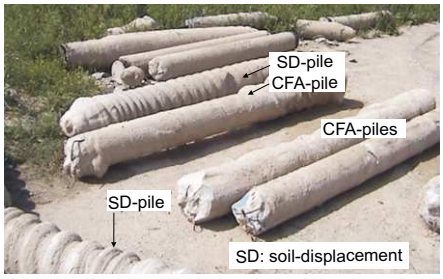

Figure 2. Excavated test piles after loading tests

2 CONTINUUM APPROACH (FEM)

Since the piles under study are cylindrical, up to a certain degree isolated and axially-loaded, the models considered within this contribution are assumed to be axisymmetric.

2.1 *FE-Mesh*

The discretisation of the soil and concrete is carried out using four-noded elements. The spatial discretization of the soil includes about 630 elements. The geometry of the model with the model's dimensions is shown in Fig. 3. The pile has a conical shaped base and a shaft diameter corresponding to test pile dimensions. The model consists of up to 6 soil layers which allows to vary densities and initial properties with depth to fit the real test conditions.

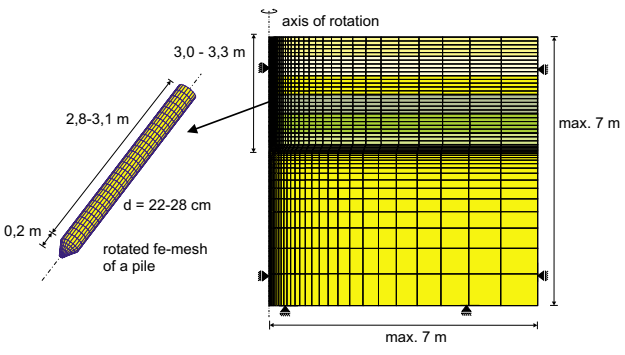

Figure 3. Axisymmetric FE-model

2.2 *Constitutive models*

Constitutive models are generally used to model the stress-strain behaviour of sand. Within this study the Drucker Prager/Cap model as implemented in the FE-code ABAQUS has been used. In order to capture the phenomenon of densification (plastic volume contraction due to isotropic stressing) a yield cap is used to close the yield surface of the classical Drucker/Prager cone surface (Fig. 4).

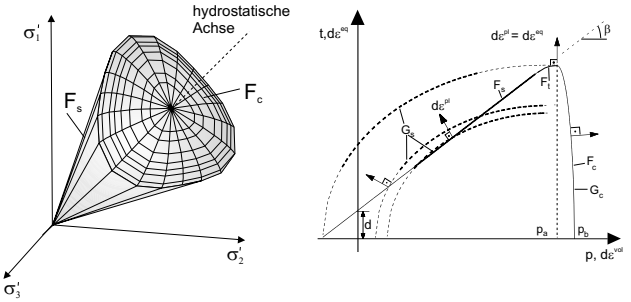

Figure 4. Drucker-Prager/Cap yield surfaces in the principal stress state and in the deviatoric stress plane

The constitutive model for the sand uses two main yield surface segments consisting of the perfectly plastic shear failure surface F_s and the compression cap yield surface F_c as shown in Fig 4.

$$F_s = t - p \cdot \tan\beta - d = 0 \tag{1}$$

$$F_c = \sqrt{(p - p_a)^2 + (R \cdot t)^2} - R \cdot (d + p_a \cdot \tan\beta) = 0 \tag{2}$$

Changes of stress inside the yield surfaces cause only elastic deformations while changes of stress on the yield surfaces cause plastic deformations. The shear failure surface is perfectly plastic whereas volumetric plastic strains cause hardening or softening of the cap. The cap hardening/softening law used within the simulations was derived from hydrostatic triaxial compression test results.

The plastic flow is defined by the non-associated flow potential G_s of the shear surface and the associated flow potential G_c of the cap (Fig. 4). The parameters β and d can be derived from the angle of friction φ' and the cohesion c' (in this case c' = 0 kN/m^2) of the soil. A more detailed description oft the soil model and how this model is used for other purposes is given in Katzenbach et al., 2003.

2.3 *Shearzone between pile and soil (interface elements)*

The mobilisation and magnitude of the ultimate shaft friction is controlled by the behaviour of a thin zone, close to the interface between pile shaft and soil. This shearzone is subjected to plastic straining similar to a simple shear mode. Depending on the soil state after pile installation and the soil characteristics within the shearzone, the soil can exhibit dilative or contractive behaviour. The tendency of the shearzone to change it's volume is influenced by the "elastic" behaviour of the surrounding soil which in a certain way acts as a constraint (compare Fig. 5, based on Wernick, 1978).

Failure at the interface between pile and soil can be modelled in two ways (Fig. 6): a) failure due to sliding between soil and pile surface, b) failure that takes place inside the soil surrounding the pile.

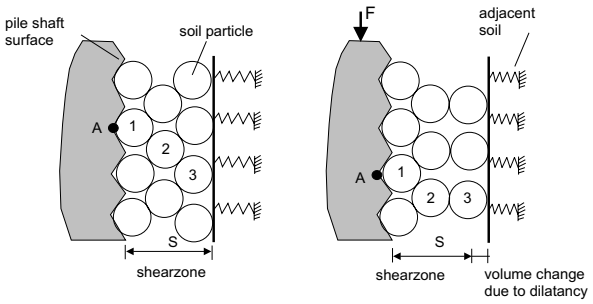

Figure 5. Pile-soil interaction, shearzone detail

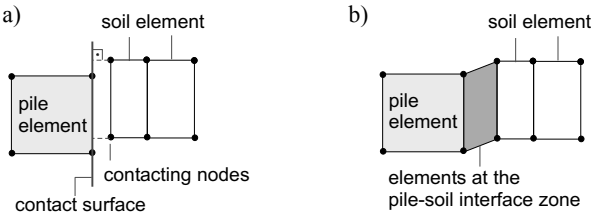

Figure 6. FE-modelling of pile-soil interaction zone (shearzone)

Based on laboratory shear box tests the shearzone between pile and sand can be extended to a small restricted area adjacent to the pile shaft than exactly being placed at the materials contact surfaces (Reul 2000). In the present study therefore a special interface element has been considered as depicted in Fig. 6b. The element is located between the pile and the soil with a width chosen 20% of the pile diameter. The classical Mohr-Coulomb constitutive model is customized to account for progressive mobilization (hardening and softening) of the soil shear strength parameter φ′ and the dilatation angle ψ within this interface element. This approach is similar to those reported in Potts & Zdravkovic, 1999 and Sarri, 2001. Each yield criterion (Mohr Coulomb line) can be considered as the current yield surface during a process of hardening and softening. As state variable to define the material behaviour the equivalent plastic strain ε^{pl} was selected (Fig. 7). The mobilized shear strength parameter φ' is expressed as function of the equivalent plastic strain magnitude (Hibbitt et al. 1998):

$$\varepsilon^{pl} = \sqrt{\frac{2}{3}\varepsilon_{ij}^{pl}\varepsilon_{ij}^{pl}} \tag{3}$$

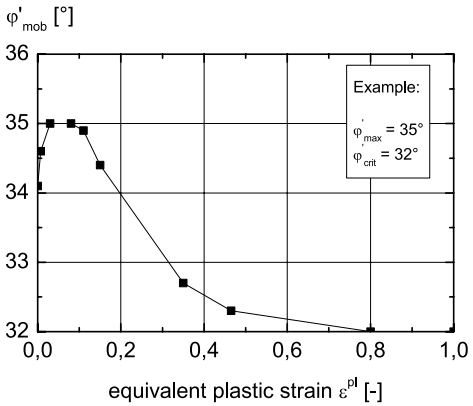

Figure 7. Friction angle φ'_{mob} in dependency of equivalent plastic strain

The angle of dilatancy is calculated according to Bolton (1986), resulting from the mobilized friction angle φ'_{mob} and the friction angle at critical state φ'_{crit}.

$$\psi = \frac{(\varphi'_{mob} - \varphi'_{crit})}{0.8} \quad (4)$$

2.4 *Accounting for soil displacement*

During the installation of screwed piles soil is displaced horizontally, densified and prestressed. An assumption on how the alteration of relative density around a soil displacement pile might qualitatively be, is given in Fig. 8.

To quantify this relationship cone penetration testing (CPT) before and after pile installation was used. Fig. 9 shows the relation between $q_{c,0}$, representing the measured cone resistance before pile installation and q_c, representing the cone resistance measured after pile installation.

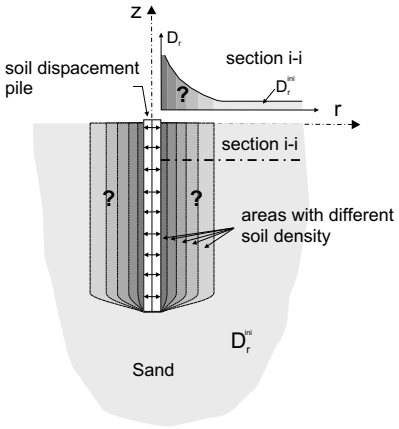

Figure 8. Assumed distribution of relative densities around a soil displacement pile

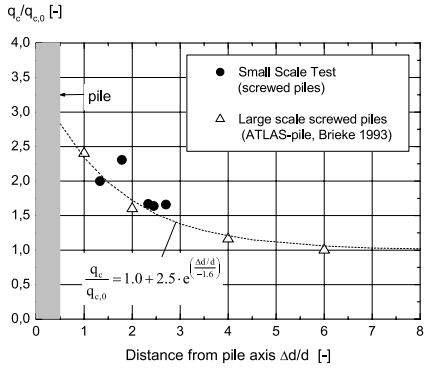

Figure 9. Decrease of cone resistance in dependency of the distance from the pile shaft

The measured cone resistance q_c after pile installation was used to assess the relative Density D_r by correlations given in DIN 4094. The value of D_r was used to assess the distribution of φ', E and ψ in dependency of the distance from the pile shaft and the medium stress level p', using equation (5) according to Bolton, 1986 and equation (6) according to Van Impe, 1986:

$$\varphi' = 3 \cdot \left[D_r \cdot \left(5{,}4 - \ln\left(\frac{p'}{p_{atm}} \right) \right) - 1 \right] + \varphi'_{crit} \quad (5)$$

with $p_{atm} = 100$ kN/m^2

$$E = \alpha_i + \beta_i \cdot q_c \quad (6)$$

with $\alpha_i = 0$, $\beta_i = 3$ for $q_c \le 5$ MN/m^2 and $\alpha_i = 7.5$, $\beta_i = 1.5$ for 5 MN/m$^2 \le q_c \le 30$ MN/m^2. The angle of dilatancy was calculated according to equation 4 with $\varphi'_{mob} = \varphi'$.

The modified horizontal stress state due to soil displacement was simulated by adjusting the lateral earth pressure coefficient during the generation of the inital stress state:

$$K = \frac{\sigma_h}{\sigma_v} \quad (7)$$

The values considered within the simulation were in the range from K = 1.0 to 1.2 and do correspond to values given in Aboutaha et al., 1993 and Rackwitz, 2003 for different types of model tests with soil displacement piles.

Parameters of the sand being used within the numerical modeling of a CFA-pile are summarized in Tabel 1.

Table 1. Properties of the sand (Drucker-Prager/Cap model)

Parameter	Unit	Sand, loose	Sand, med. dense
Relative Density D_r	-	0.2	0.45
Young's modulus E	Mpa	12	23
Poisson's ratio υ	-	0.3	0.3
Coeff. of earth pressure K_0	-	0.46	0.38
Buoyant unit weight γ′	kN/m^3	8	8
Angle of friction φ′	°	33	38
Cohesion c′	kPa	0	0
Interface zone (Modified Mohr-Coulomb model)			
Angle of friction φ′	°	32	38
Angle of friction φ'_{crit}	°	32	32
Cohesion c′	kPa	0	0
Angle of dilatancy ψ	°	(eq. 4)	(eq. 4)

For the simulation of a displacement pile K_0 was replaced by K (according to equation 7) to account for the altered stress state around the displacement pile.

3 SIMULATION PROCEDURE

Pile installation and testing has been modeled by the following simulation steps:

- initial stress state
- excavate soil according to pile dimensions
- allow soil to expand or relax due to liquid concrete pressure
- reduce concrete pressure to zero and install concrete pile elements with final stiffness
- apply gravity loading on the concrete pile elements
- subsequent loading of the pile (displacement driven)

For the initial horizontal stress distribution a K_0 stress field has been generated for bored piles without soil displacement. The horizontal stresses $\sigma_x = \sigma_y$ are derived from the overburden stresses σ_z by applying the factor of K_0.

$$\sigma_z^{(z)} = \int_0^z \gamma' dz \quad (8)$$

$$\sigma_x^{(z)} = \sigma_y^{(z)} = K_0 \cdot \sigma_z \quad (9)$$

K_0 was chosen to be constant for all single soil layers according to $K_0 = 1 - \sin\varphi'$. Simulations where soil displacement is considered start with an already installed pile and an adjusted K value as stated in section 2.4.

4 RESULTS OF NUMERICAL SIMULATION

The load applied at the pile head is split into shaft resistance and base resistance and is compared with the experimental results.

In Fig. 10 the results of numerical simulations are exemplarily given for a conventional CFA pile and a soil displacement pile. The increase in horizontal stresses due to the installation of a displacement pile was considered within the numerical model by a value of K being equal to 1.2, according to stress measurements during the pile installation within the testing container of model tests (Katzenbach et al., 2004). The initial soil density around the two piles was comparable with a cone resistance (CPT) of $2{,}5\ \mathrm{MN/m^2} \le q_c \le 5\mathrm{MN/m^2}$.

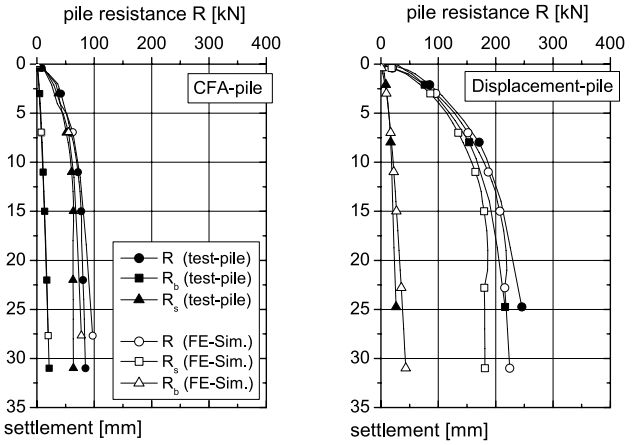

Figure 10. Comparison FE-Simulation and test pile behaviour (R: pile resistance, R_b: base resistance, R_s: shaft resistance)

In Fig. 11 the distribution of skin friction from FE-simulations is shown. The variation of values is influenced by the variation of soil density at the beginning of the simulation.

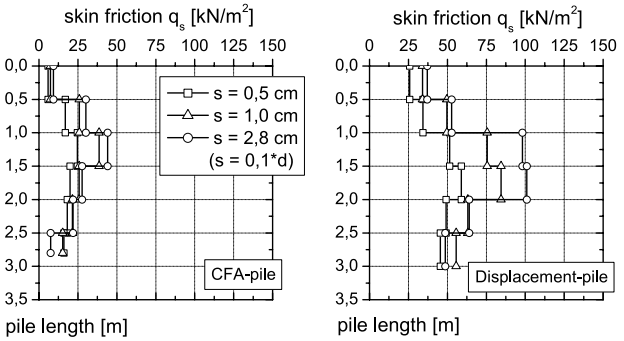

Figure 11. Skin friction along the pile shaft (numerical simulation)

However the graphs show that a soil displacement pile is leading to an increase of pile shaft capacity of more than 100% in the lower pile section. The skin friction obtained for CFA piles within the numerical simulations corresponds to:

$$q_s = \alpha_b \cdot q_c \qquad (10)$$

With $\alpha_b = 0.008$ and q_c in $\mathrm{MN/m^2}$ as stated in DIN 1054. The higher values of skin friction for the displacement piles can be derived in the same manner when relying on cone penetration results evaluated from tests performed after the installation of a displacement pile. The procedure of using CPT also after pile installation becomes even more important when installing displacement piles in layered soils and when using a soil displacement that is not kept constant over the entire pile length.

5 CONCLUSIONS

Numerical analysis were used to assess the load-bearing behaviour of single model piles in sand. By introducing an interface element between pile shaft and surrounding soil, based on the Mohr-Coulomb criteria with a progressive mobilisation of the shear strength, it was possible to simulate the observed pile bearing behaviour of bored and screwed piles. However considerably more efforts are necessary to accurately investigate the influence of different degrees of soil displacement during the installation of piles on the characteristics of the surrounding soil. This would enable to set up reliable criteria for the simulation of displacement piles also under the aspect of predicting the load bearing behaviour of more complicated foundation structures as e.g. Combined Pile-Raft Foundations.

REFERENCES

Aboutaha, M., De Roeck, G. and Van Impe, W.F., 1993. Bored versus displacement piles in sand – experimental study. *Deep Foundations on Bored and Auger Piles, (Ed.: Van Impe), Balkema, Rotterdam,* 157-162

Bolton, M.D., 1986. The strength and dilatancy of sand. *Géotechnique 36, No. 1,* 65-78

Brieke, W. 1993. Vergleich der Tragfähigkeit unterschiedlicher Pfahlsysteme. *Franki Grundbau GmbH, Neuss*

DIN 4094, Juni 2002. Baugrund • Felduntersuchungen. *Normenausschuss Bauwesen (NABau) im DIN Deutsches Institut für Normung e.V.*

DIN 1054, Januar 2003. Baugrund • Sicherheitsnachweise im Erd- und Grundbau. *Normenausschuss Bauwesen (NABau) im DIN Deutsches Institut für Normung e.V.*

Hibbit H.D., Karlsson, B.J. and Sorensen, 1998.ABAQUS Theory Manual, Version 5.8

Katzenbach, R., Schmitt, A. and Turek, J., 2003. Assessing Settlement of High-Rise Structures by 3D Simulations. *Journal of Computer-Aided Civil and Infrastructure Engineering, Special Issue on Computing in Civil and Building Engineering, (submitted for review)*

Katzenbach, R., Schmitt, A., Furmanovicius, L., Nicholson, D., Dinesh, P., Powell, J.M., Skinner, H. and Hamelin, J.-P., 2004. Neue Techniken für Ortbetonverdrängungspfähle. *Vorträge zum 11. Darmstädter Geotechnik-Kolloquium am 18. März 2004. Mitteilungen des Institutes und der Versuchsanstalt für Geotechnik der Technischen Universität Darmstadt, Heft 68,* 99-116

Potts, D.M. and Zdrackovic, L., 1999. Finite element analysis in geotechnical engineering theory. *Thomas Telford, ISBN 07-277-27532*

Rackwitz, F., 2003. Numerische Untersuchung zum Tragverhalten von Zugpfählen und Zugpfahlgruppen in Sand auf der Grundlage von Probebelastungen. *Veröffentlichungen des Grundbauinstitutes der Technischen Universität Berlin, Heft 32*

Reul, O., 2000. In-situ-Messungen und numerische Studien zum Tragverhalten der Kombinierten Pfahl-Plattengründung, *Mitteilungen des Institutes und der Versuchsanstalt für Geotechnik der Technischen Universität Darmstadt,* Heft 53

Sarri, H., 2001. Pali trivellati in sabbia soggetti a carico assiale: modellazione fisica e numerica. *Politecnico di Torino, Tesi di dottorato.*

Van Impe, W.F., 1986. Evaluation of deformation and bearing capacity parameters of foundations, from static CPT-results. *Fourth Int. Geotechnical Seminar – Field Instrumentation and In-Situ Measurements, Nanyang Technological Institute, Singapore, 25-27 November 1986*

Wernick, E., 1978. Tragfähigkeit zylindrischer Anker in Sand unter besonderer Berücksichtigung des Dilatanzverhalten. *Veröffentlichungen des Institutes für Bodenmechanik und Felsmechanik der Universität Fridericiana in Karlsruhe, Heft 75*